

Supplementary Information

Catalytic mechanism of a retinoid isomerase essential for vertebrate vision

Philip D. Kiser¹, Jianye Zhang¹, Mohsen Badiie², Qingjiang Li², Wuxian Shi^{3,4}, Xuewu Sui¹, Marcin Golczak¹, Gregory P. Tochtrop² and Krzysztof Palczewski¹

Affiliations

¹ Department of Pharmacology, Cleveland Center for Membrane and Structural Biology, School of Medicine, Case Western Reserve University, Cleveland, OH 44106

² Department of Chemistry, Case Western Reserve University, Cleveland, OH 44106

³ National Synchrotron Light Source, Brookhaven National Laboratory, Upton, NY 11973

⁴ Case Center for Synchrotron Biosciences, School of Medicine, Case Western Reserve University, Cleveland, OH 44106

SUPPLEMENTARY RESULTS

Supplementary Table 1. X-ray data collection and refinement statistics

	Emixustat	MB-001
Data collection[†]		
Space group	<i>P6₅</i>	<i>P6₅</i>
Cell dimensions		
<i>a</i> , <i>b</i> , <i>c</i> (Å)	175.89, 175.89, 86.53	175.64, 175.64, 86.61
α , β , γ (°)	90, 90, 120	90, 90, 120
Resolution (Å)	50-1.8 (1.91-1.8)*	50-2.39 (2.53-2.39)
<i>R</i> _{merge} (%)	11.7 (164.5)	19.9 (157.8)
<i>I</i> / σ <i>I</i>	12.7 (1.1) [‡]	9.7 (0.96)
Completeness (%)	99.5 (97.1)	99.2 (94.8)
Redundancy	8.9 (7.1)	7.1 (4.7)
Refinement		
Resolution (Å)	47.9-1.8	47.9-2.39
No. reflections	132075	56801
<i>R</i> _{work} / <i>R</i> _{free} (%)	16.5/19.6	19.6/23.6
No. atoms	9390	8780
Protein	8310	8291
Ligand/ion	iron: 2	iron: 2
	emixustat: 38	MB-001: 44
	palmitate: 36	palmitate: 36
Water	1004	401
<i>B</i> -factors (Å ²)	33	47
Protein	32	47
Ligand/ion	iron: 23	iron: 39
	emixustat: 39	MB-001: 64
	palmitate: 43	palmitate: 55
Water	44	45
R.m.s. deviations		
Bond lengths (Å)	0.014	0.009
Bond angles (°)	1.55	1.40

[†] Each data set was collected from a single crystal

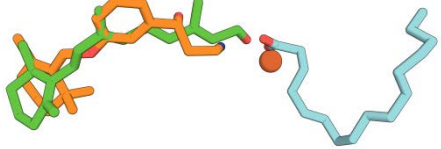
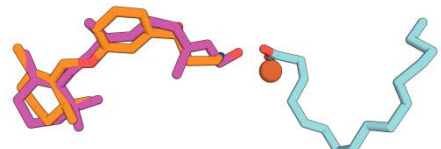
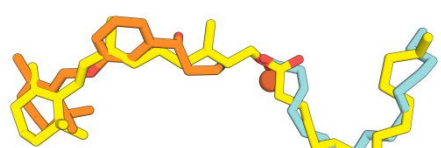
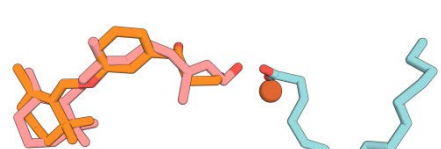
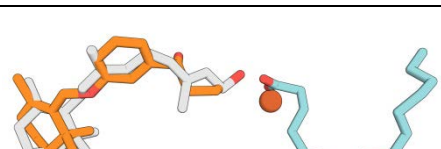
* Highest-resolution shell is shown in parentheses.

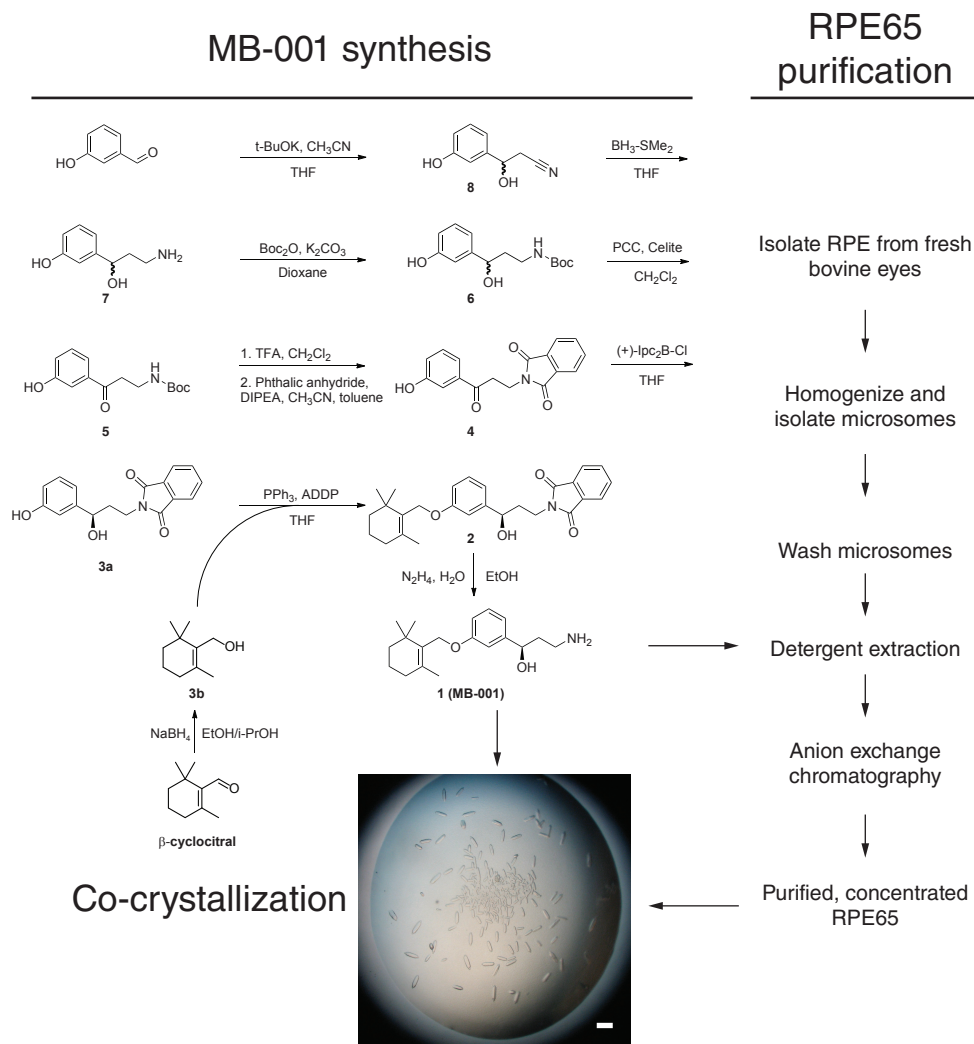
[‡] *I*/ σ *I* values for the next highest resolution shells of data for the emixustat (2.05-1.91 Å) and MB-001 (2.71-2.53 Å) data sets were 2.4 and 1.8, respectively.

Supplementary Table 2. Fe-ligand bond angles vs. ideal values for angles that differ between octahedral and trigonal bipyramidal geometries. Values in columns A and B are the specified bond angles for chains A and B, respectively, of the RPE65-emixustat complex. The smaller angle discrepancy for trigonal bipyramidal coordination indicates that it is the best description of the iron center geometry.

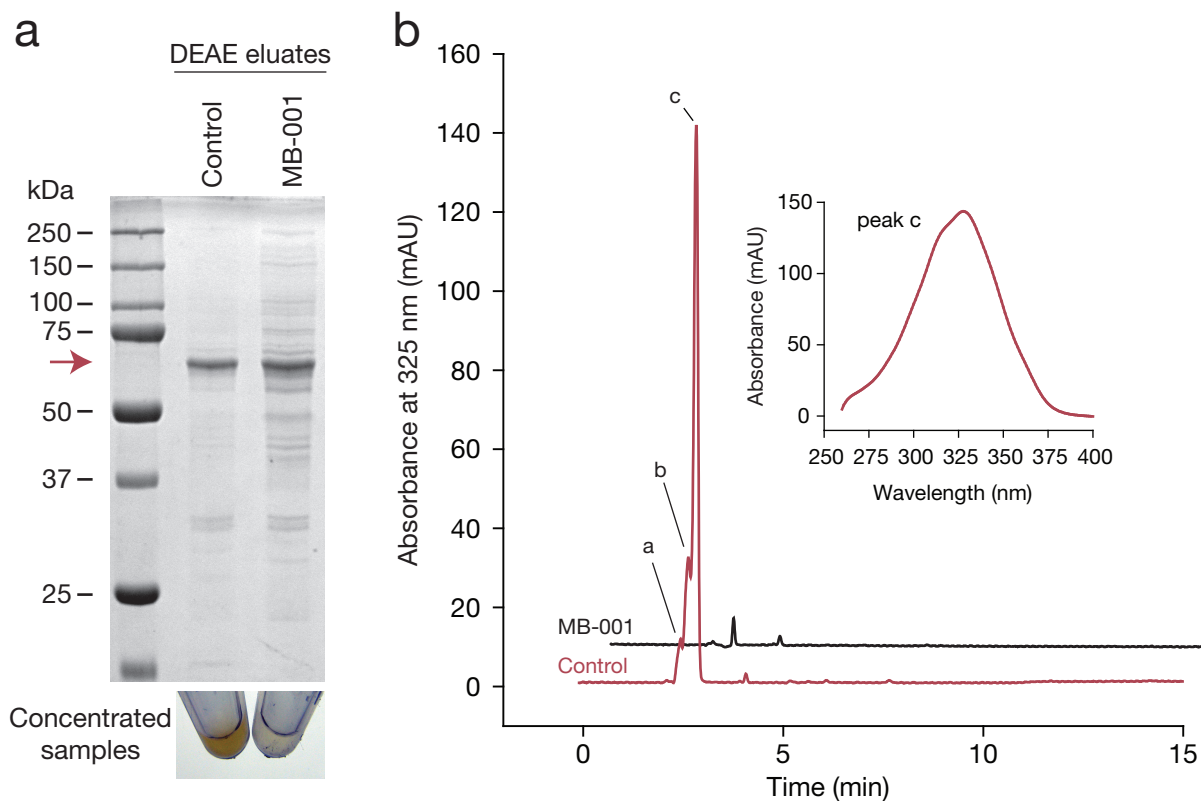
	A	B	Octahedral (ideal, absolute difference)	Trigonal bipyramidal (ideal, absolute difference)
O-Fe-N ϵ 180	113°	114°	90°, 23.5°	120°, 6.5°
O-Fe-N ϵ 313	149°	149°	180°, 31°	120°, 29°
N ϵ 180-Fe-N ϵ 313	98°	98°	90°, 8°	120°, 22°
Sum of angle discrepancies	--	--	62.5°	57.5°

Supplementary Table 3. Retinoid ligand docking into the RPE65 active site. MB-001 (orange), palmitate (cyan) and iron (brown sphere) are shown in the panels on the right to provide a frame of reference.

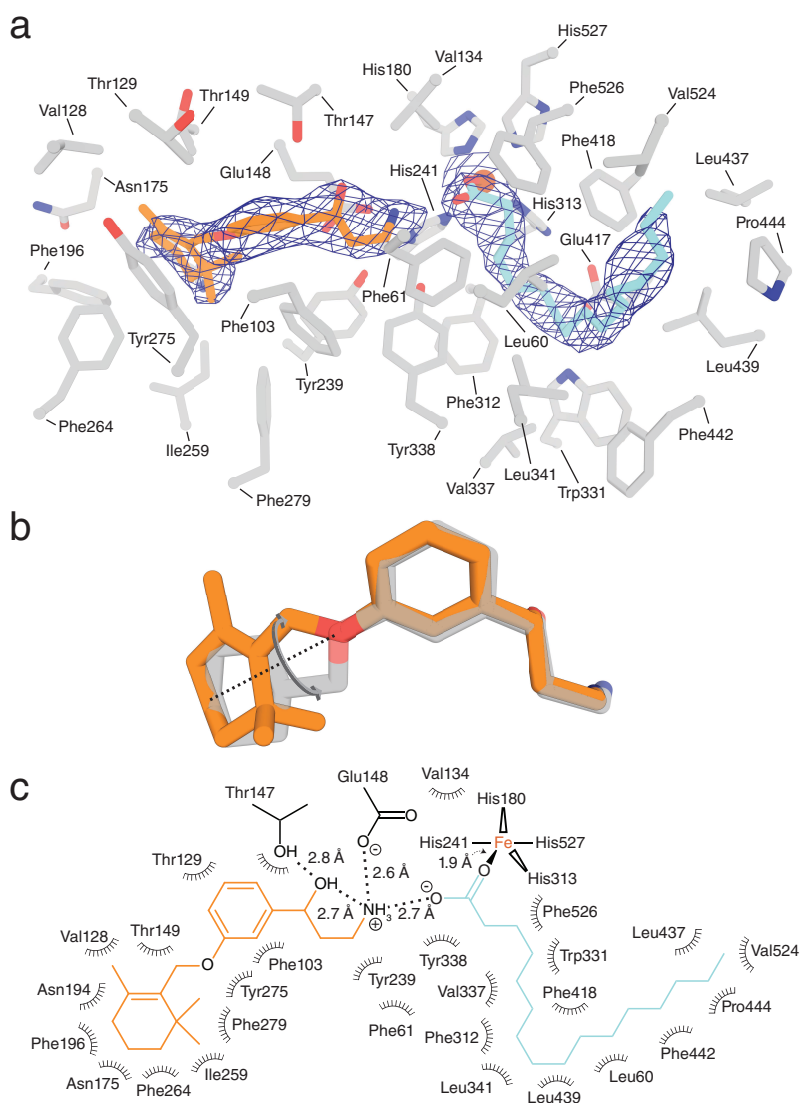
Structure	Rotatable bonds	Docking score for top two poses (kcal/mol)	Structure (top pose)
all-<i>trans</i>-retinol	Polyene single bonds	1. -9.5 2. -8.6	
11-<i>cis</i>-retinol	Polyene single bonds	1. -10.4 2. -9.9	
all-<i>trans</i>-retinyl palmitate	Polyene single bonds	1. -10.7 2. -9.9	
all-<i>trans</i>-retinol	Polyene single bonds and 11-12, 13-14 double bonds	1. -10.1 2. -9.8	
11-<i>cis</i>-retinol	Polyene single bonds and 11-12, 13-14 double bonds	1. -10.1 2. -9.9	



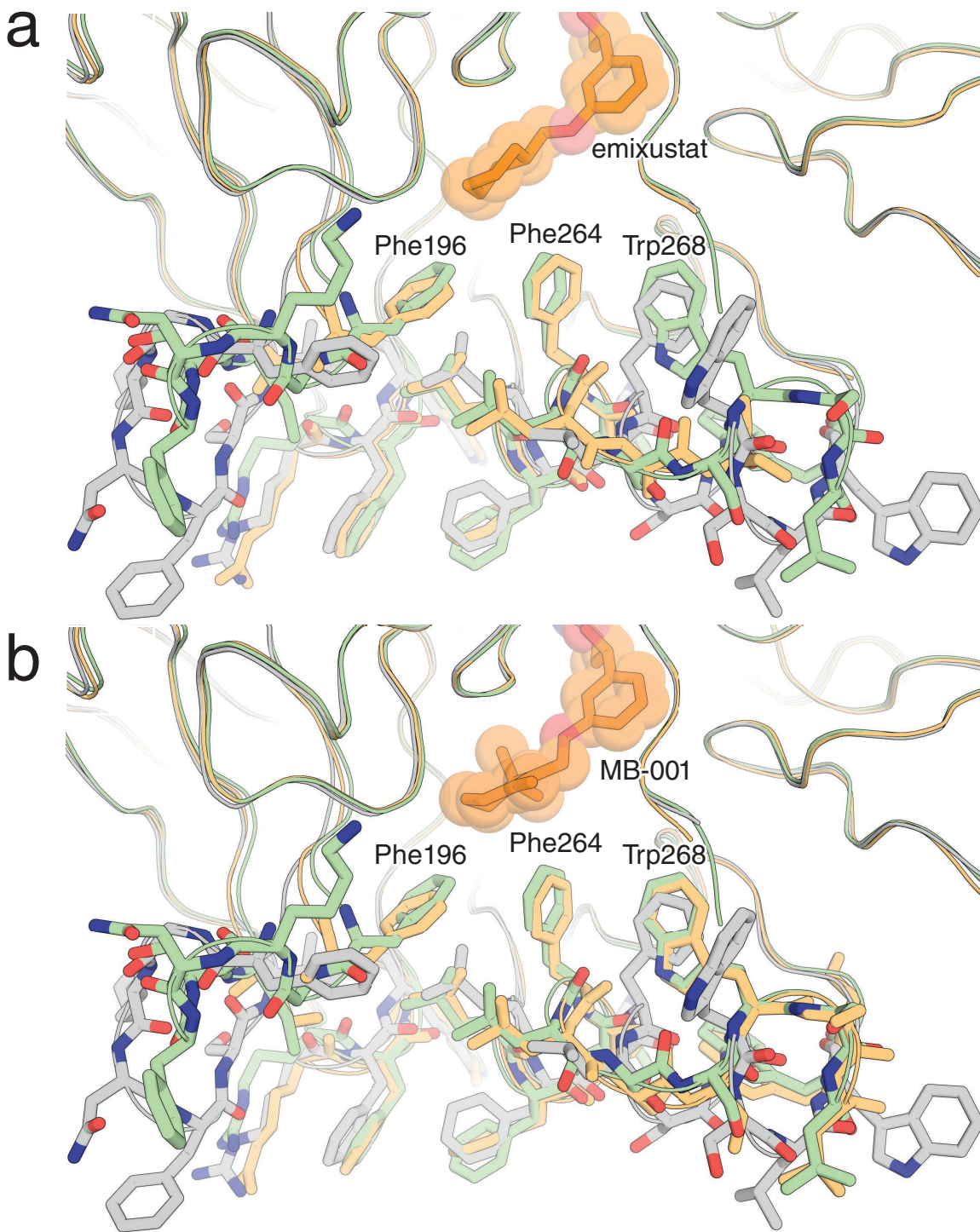
Supplementary Figure 1. Preparation of RPE65 and MB-001 for crystallization studies. MB-001 was synthesized as described in the online methods. RPE65 purification was performed essentially as described previously except that C_8E_6 was used in place of C_8E_4 as the detergent¹. MB-001 was added to the RPE65-containing samples at the detergent extraction step of purification as well as to the final purified sample just prior to initiation of the crystallization trials. The same procedure was used for the emixustat-RPE65 crystallization experiments. The scale bar in the image of the crystals obtained from the procedure indicates a horizontal length of 150 μm .



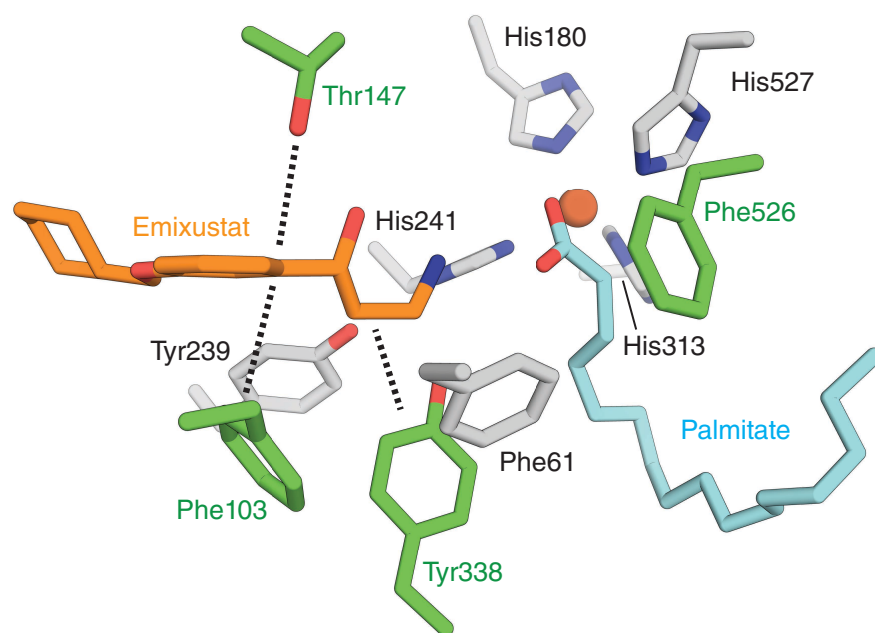
Supplementary Figure 2. Characterization of RPE65 purified in the presence of MB-001. (a) SDS-PAGE of RPE65 purified in the presence and absence of MB-001. The red arrow indicates the position of the RPE65 band. RPE65 purified in the presence of MB-001 loses its typical red-brown color, which is maintained in the solvent-only control (DMF). (b) HPLC analysis of the retinyl ester content of purified RPE65 samples. The peaks corresponding to different retinyl esters (C20, C18 and C16 for a, b and c, respectively) are absent in RPE65 samples prepared in the presence of MB-001. The inset shows the absorbance spectrum for peak “c”, which along with its retention time confirms its identity as all-*trans*-retinyl palmitate.



Supplementary Figure 3. Crystal structure of RPE65 in complex with MB-001 and its comparison to the emixustat-bound structure. (a) Unbiased 2Fo-Fc electron density map calculated after the initial rigid body refinement prior to inclusion of ligands in the structural model. The map is shown within 2 Å of the bound MB-001 (orange sticks) and palmitate (cyan sticks) ligands. Residues within 4.5 Å of the bound ligands are shown as grey sticks. (b) Comparison of the MB-001 and emixustat binding conformations. The 3-amino-1-phenylpropan-1-ol moieties exhibit similar binding positions and conformations. A 180° rotation of the phenoxy bond distinguishes the binding modes for the aliphatic rings of MB-001 and emixustat. (c) Two-dimensional interaction diagram for the MB-001 and palmitate ligands. Polar interactions are shown with dashed lines. Residues participating in non-dipolar interactions are shown as spiked arcs.



Supplementary Figure 4. Conformational differences between residues of the membrane-entry port in close proximity to the aliphatic rings of the inhibitors. For (a), emixustat-bound structure, and (b), MB-001-bound structure, the inhibitor-bound structure is shown in light orange, the originally determined delipidated RPE65 structure (PDB accession code 3FSN) in grey and the lipid-embedded “active” structure (PDB accession code 4F2Z) in light green. In both inhibitor structures, residues that make up the membrane entry port including Phe196, Phe264 and Trp 268 adopt conformations similar to those observed for the lipid-embedded “active” RPE65 structure.



Supplementary Figure 5. RPE65 active site residues critical for isomerization activity and stereoselectivity. Residues represented as green sticks were shown to control isomerization stereoselectivity whereas those shown in grey are important for the overall level of isomerization activity of the enzyme.

Supplementary Movie 1. Binding site locations and electron density maps for the retinoid-mimetic inhibitors, emixustat and MB-001, and palmitate. For clarity only the main cavities are shown in the surface representation displayed in the first part of the movie. Sticks within 4.5 Å of the ligands are shown in the second part of the movie. Final sigma A-weighted 2Fo-Fc electron density maps are shown as blue mesh.

Supplementary Movie 2. Catalytically important features of the RPE65 active site. This movie illustrates the active site features described in Fig. 4, b and c including the retinoid-binding site constriction at the C11 position as well as the putative nucleophilic water molecule. The binding position for 11-*cis*-retinol shown in the movie is that predicted from computational docking as shown in Supplementary Table 3 (11-*cis*-retinol with rotatable polyene single bonds).

Reference

1. Kiser, P.D., Golczak, M., Lodowski, D.T., Chance, M.R. & Palczewski, K. Crystal structure of native RPE65, the retinoid isomerase of the visual cycle. *Proc. Natl. Acad. Sci. U.S.A.* **106**, 17325-30 (2009).